NJC

Accepted Manuscript

This is an *Accepted Manuscript*, which has been through the Royal Society of Chemistry peer review process and has been accepted for publication.

Accepted Manuscripts are published online shortly after acceptance, before technical editing, formatting and proof reading. Using this free service, authors can make their results available to the community, in citable form, before we publish the edited article. We will replace this *Accepted Manuscript* with the edited and formatted *Advance Article* as soon as it is available.

You can find more information about *Accepted Manuscripts* in the Information for Authors.

Please note that technical editing may introduce minor changes to the text and/or graphics, which may alter content. The journal's standard Terms & Conditions and the Ethical guidelines still apply. In no event shall the Royal Society of Chemistry be held responsible for any errors or omissions in this *Accepted Manuscript* or any consequences arising from the use of any information it contains.

ROYAL SOCIETY OF CHEMISTRY

www.rsc.org/njc

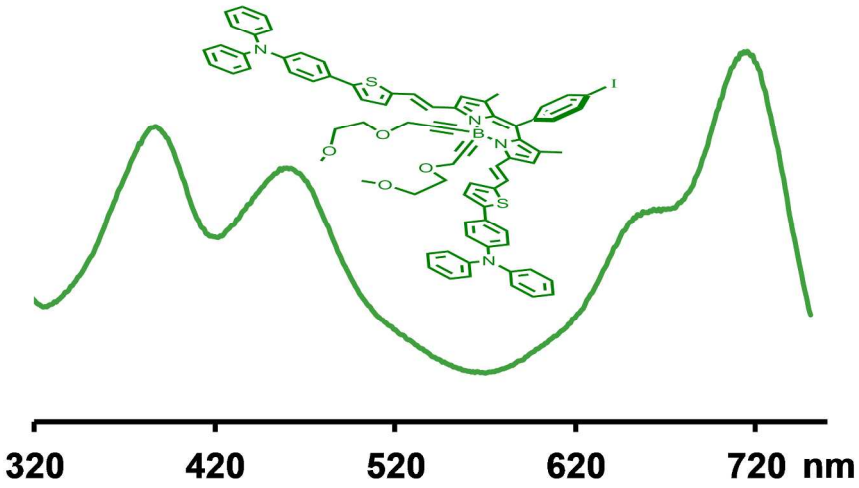

210x122mm (300 x 300 DPI)

New Journal of Chemistry Accepted Manuscript

Journal Name

RSCPublishing

ARTICLE

Photovoltaic Performance of Novel Push-Pull-Push Thienyl-Bodipy Dyes in Solution-processed BHJ-Solar Cells

Cite this: DOI: 10.1039/xoxxoooooox

Received ooth January 2012,
Accepted ooth January 2012

DOI: 10.1039/xoxxoooooox

www.rsc.org/

Alexandra Sutter,[a] Pascal Retailleau,[b] Wei-Ching Huang,[c] Hao-Wu Lin,[c,*] and Raymond Ziessel[a,*]

Abstract. This work explores the synthesis of extended dipyrromethene dyes engineered from thiophene-linked triphenylamine modules in order to favor pronounced charge transfer within the dyes and to enable their use in solar cells. We found that these soluble dyes absorb up to 760 nm in solution and 850 nm in thin films. An effective charge transfer absorption band was found around 460 nm. In the crystal lattice, molecules are organized in layers separated by 3.50 Å with pronounced π-π stacking and S···S interactions. The electroactivity of the dyes indicates that electron injection in $PC_{71}BM$ is feasible. Bulk heterojunction solar cells based upon dyes **1** and **2** in an optimized device structure ITO/Ca/**1** or **2**:$PC_{71}BM/MoO_3$/Ag provide a power conversion efficiency of about 1.5% after thermal annealing.

1. Introduction

The fabrication of solar energy conversion devices is a major contemporary interest of the general scientific community due to their promise as low-cost and renewable energy sources.[1] Production of organic solar cells (OSC's) by solution-processing techniques is a promising technology for cheap and flexible panels.[2] Usually the photoactive layer is made of a blend of a small and highly colored organic molecule or soluble low band-gap polymer considered as the electron donor and a soluble fullerene derivative able to accept the photo-excited electron.[3] Note that small molecules can be co-evaporated with the acceptor under ultra-high vacuum to form the photoactive layer. In both cases a nanophase-segregation between the donor and acceptor is mandatory to provide high efficiency.[4] Impressive photoconversion efficiencies of 8.9%[5] to above 10%[6] were recently reached using small molecules and both technological approaches.

A key factor for the success of OSC's is the nature of the dyes which absorb the photons, allow diffusion of the excitons in the thin layer and finally promote charge separation at the interface with the acceptor in the bulk-heterojunction (BHJ).[7] Many dyes have been screened including oligothiophenes,[8] diketopyrrolopyrroles (DPP),[9] mixed DPP-TAT dumbell-shaped scaffoldings (TAT for triazatruxene),[10] squaraines,[11] hexabenzo-coronenes,[12] merocyanines,[13] donor-acceptor oxoindanes,[14] thiadiazolo-bithienyls,[15] benzodithiophenes,[16] benzothia-diazoles,[17] and Bodipy-thienyls.[18,19]

Borondipyrromethene (Bodipy) dyes are attractive in organic photovoltaic cells (OPVs)[18,19,20] and dye-sensitized solar cells (DSCCs)[21] mostly because many chemical tools allow tailoring at will of the optical and redox properties.[22] Consequently, several substituted Bodipy dyes were tested as sensitizers in BHJ solar cells with photoconversion efficiencies spanning from 0.9 to 4.7%. Some of these Bodipys were constructed with vinyl side arms in the 3,5-substitution positions, ensuring extended delocalization pathways in the ground state and intense absorption in the visible portion of the electromagnetic spectra. In some cases, these vinyl groups were elaborated with strong donor groups like triazatruxene providing good charge transport in the active layer and a good match with the solar spectrum.[20b] Interestingly, mixing of similar dyes allowed extension of the photon absorptivity of the device and ensured better photon to current conversion.[20b] The use of thiophene-grafted Bodipys markedly improved the efficiency, mostly due to high mobility of hole and electron inside the thin photoactive layer.[19] It has further been demonstrated that a very high open-circuit voltage could be achieved by linking triphenylamine (TPA) fragments in the 2,6-susbtitution positions of a Bodipy framework.[20c]

Herein we describe novel extended Bodipy dyes built from both TPA-thiophene (push) modules in a conjugated situation with a 3,5-substituted Bodipy (pull) skeleton. The idea was to increase the electronic density on the thiophene site in order to favour charge transfer with the electron withdrawing Bodipy module without perturbing to a large extent the electrochemical gap (HOMO/LUMO). The target dyes were prepared as shown in

New Journal of Chemistry Accepted Manuscript

Scheme 1. The rationales for the fluorine group substitution rely on our previous work, where we increase the steric bulkiness around the boron center to avoid aggregation process and increase the solubility and chemical and photochemical stability of the dyes.[23]

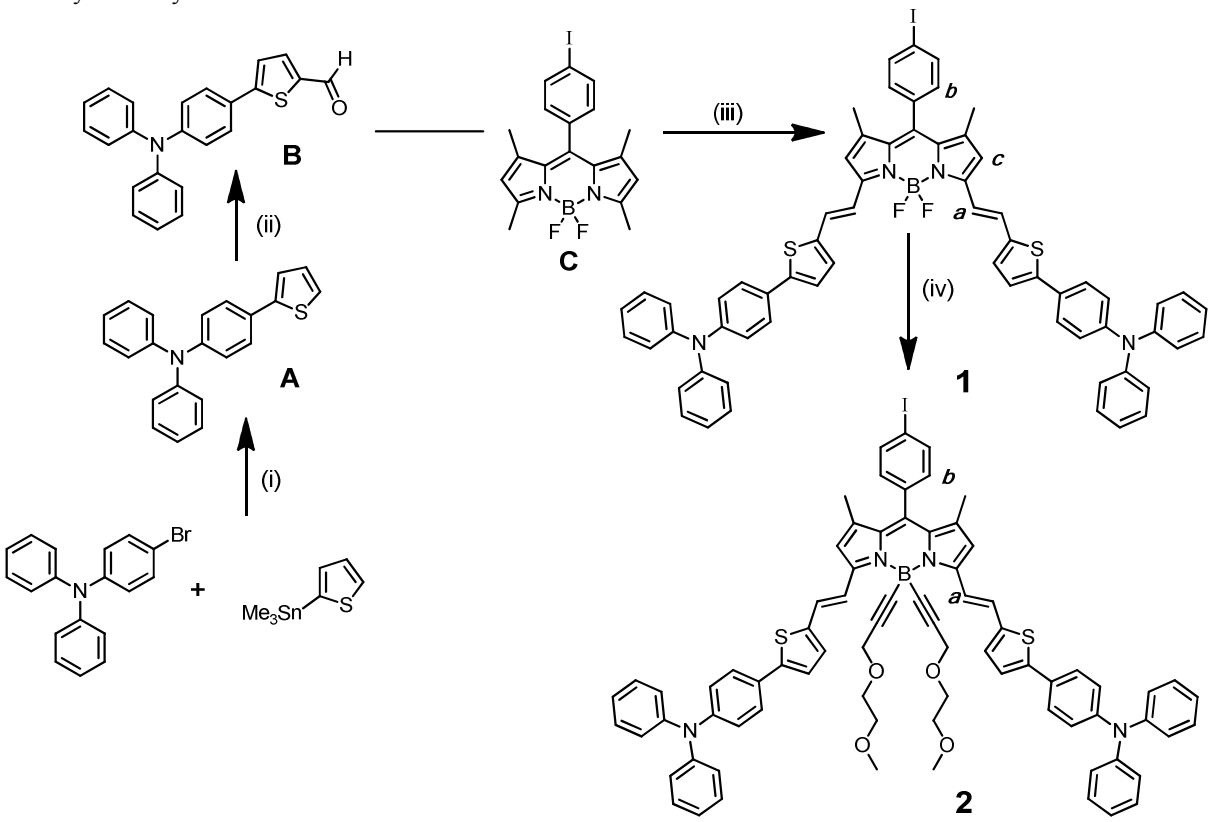

Scheme 1. Keys : (i) $[Pd(PPh_3)_4]$ (6 mol %), toluene, 110°C, overnight (15h) ; ii) a) $POCl_3$ (1.1 eq), DMF (1.4 eq), 0°C, 1h, b) compound **A**, 1,2-dichloroethane, 85°C, overnight (15h) ; iii) compound **C** (1 eq), compound **B** (3 eq), piperidine, *p*-TsOH, toluene, reflux, Dean-Stark apparatus, overnight (15h) ; iv) a) 3-(2-methoxyethoxy)prop-1-yne (4 eq), EtMgBr (3.5 eq), THF, 60°C, 2h, b) compound **1** (1 eq), THF, 60°C, overnight (15h).

2 Experimental Part.

2.1 General methods

All chemicals were obtained from commercial sources (Sigma Aldrich, Alfa Aesar) and used, unless otherwise stated, without further purification. All anhydrous reactions were performed under a dry atmosphere of argon using standard Schlenk techniques. THF was distilled over sodium and benzophenone under an argon atmosphere. 1, 2-dichloroethane was distilled over P_2O_5 under an argon atmosphere. DMF and thiophene were distilled over potassium hydroxide under argon.

^{1}H NMR, ^{13}C NMR and ^{11}B NMR spectra were recorded on BRUKER spectrometers with reference chemical shifts taken as $CHCl_3$ (δ = 7.26 ppm) for ^{1}H NMR, and $CDCl_3$ (δ = 77.2 ppm) for ^{13}C NMR, while the signal from the B within the borosilicate of the NMR tubes was used for ^{11}B NMR. Electronic absorption spectra were recorded using a Shimadzu UV-3600 dual-beam grating spectrophotometer with a 1 cm quartz cell. Steady-state emission and excitation spectra were recorded on a HORIBA Jobin-Yvon FluoroMax 4P spectrofluorimeter. All fluorescence spectra were corrected. The fluorescence quantum yield (Φ_{exp}) was calculated from equation (1):

$$\Phi_{exp} = \Phi_{ref}\frac{F\left[1-exp\left(-A_{ref}ln10\right)\right]n^2}{F_{ref}[1-exp(-A\,ln10)]n_{ref}^2} \quad (1)$$

Here, F denotes the integral of the corrected fluorescence spectrum, A is the absorbance at the excitation wavelength and n is the refractive index of the medium.

Tetramethoxydiisoindomethene-difluoroborate (ϕ_F = 0.51 in dichloromethane) was used as the emission reference for both compounds emitting above 650 nm.[24]

Potentials determined by cyclic voltammetry in deoxygenated CH_2Cl_2 solutions, containing 0.1 M $TBAPF_6$, at a solute concentration range of ca 1 mM and at rt. Potentials are given versus the saturated calomel electrode (SCE) and standardized vs ferrocene (Fc) as internal reference assuming that $E_{1/2}$ (Fc/Fc^+) = +0.38 V (ΔEp = 60 mV) vs SCE. The error in half-wave potentials is ±10 mV. Where the redox processes are

New Journal of Chemistry Accepted Manuscript

 This journal is © The Royal Society of Chemistry 2012

irreversible, the peak potentials (E_{ap} or E_{cp}) are quoted. All reversible redox steps result from one-electron processes unless otherwise specified.

2.2 Preparative work.

Materials. $[Pd(PPh_3)_4]$,[25] **A**,[26] **B**,[27] Bodipy **C**,[17,18] and 3-(2-methoxyethoxy)prop-1-yne[18] were synthesized according to the indicated literature procedures. The preparation of trimethyl(thiophen-2-yl)stannane was adapted from reference 25 by replacing tri-n-butylstannylchloride by trimethylstannyl-chloride.

Synthesis of 1. To a solution of Bodipy **C** (199.8 mg, 0.44 mmol) in toluene (40 mL) was added 5-(4-diphenylaminophenyl)-2-carbaldehydethiophene **B** (473.5 mg, 1.33 mmol), piperidine (1 mL) and one crystal of *p*-toluenesulfonic acid. The resulting mixture was stirred at reflux overnight using a Dean-Stark apparatus. After being cooled, the organic product was extracted into CH_2Cl_2, and washed with water and brine. The organic layer was dried over anhydrous MgSO4 and evaporated under vacuum. The crude product was purified by silica gel chromatography (from 60/40 to 50/50 Petroleum Ether/CH_2Cl_2) and recrystallized by slow evaporation of dichloromethane from a mixture of CH_2Cl_2/EtOH. The resulting crystals were collected and washed with pentane to afford a green compound (431.1 mg, 86%). ^{1}H NMR δ (ppm): (300 MHz, $CDCl_3$): δ (ppm) 7.85 (d, ^{3}J = 8.1 Hz, 2 H), 7.42-7.55 (m, 6 H), 7.01-7.36 (m, 32 H), 6.60 (s, 2 H), 1.47 (s, 6 H). ^{13}C NMR (300 MHz, $CDCl_3$): δ (ppm) 152.3, 147.8, 147.4, 146.3, 141.3, 140.8, 138.2, 134.9, 133.5, 130.7, 129.4, 129.2, 127.9, 126.7, 124.7, 123.4, 123.3, 123.2, 118.2, 117.7, 94.7, 14.9. EI-MS m/z (%)1124.1 (100). Anal. for $C_{65}H_{48}BF_2IN_4S_2$: found C, 69.31; H, 4.21; N, 4.68; calcd for $C_{65}H_{48}BF_2IN_4S_2$: C, 69.40; H, 4.30; N, 4.98.

Synthesis of 2. In a Schlenk flask, ethylmagnesiumbromide (702.8 µL, 0.80 mmol) was added to a stirred solution of 3-(2-methoxyethoxy)prop-1-yne (96.3 µL, 0.70 mmol) in anhydrous THF (5 mL). The mixture was stirred at 60 °C for 2 h under argon. The resulting anion was then transferred with a canula to a solution of **1** (225.9 mg, 0.20 mmol) in anhydrous THF (5mL). After the reaction mixture was stirred at 60 °C overnight under argon, water was added, and the solution was extracted with CH_2Cl_2. The organic phase was washed with water, dried over anhydrous $MgSO_4$ and evaporated under vacuum. The crude product was purified by silica gel chromatography (from pure CH_2Cl_2 to 98/2 CH_2Cl_2/MeOH) and recrystallized by evaporation in CH_2Cl_2/EtOH to afford a green compound 2 (198.2 mg, 75%) after washing with pentane. 1H NMR (300 MHz, $CDCl_3$) δ (ppm): 8.00 (d, ^{3}J=15.9 Hz, 2 H), 7.85 (d, J=8.3 Hz, 2 H), 7.52 (d, ^{3}J=8.6 Hz, 4 H), 6.98 - 7.33 (m, 32 H), 6.61 (s, 2 H), 4.23 (s, 4 H), 3.64 - 3.71 (m, 4 H), 3.28 - 3.35 (m, 4 H), 3.16 (s, 6 H), 1.45 (s, 6 H).^{13}C NMR (300 MHz, $CDCl_3$) δ (ppm) 151.5, 147.8, 147.2, 145.9, 141.5, 139.9, 138.2, 136.1, 135.24, 131.8, 130.8, 129.4, 127.8, 127.3, 126.7, 124.7, 123.4, 119.7, 118.5, 71.7, 68.3, 59.4, 58.8, 15.1. EI-MS m/z (%): 1312.2 (100). Anal. for $C_{77}H_{66}BIN_4O_4S_2$: found C, 70.22; H, 4.86; N, 4.01; calcd for $C_{77}H_{66}BIN_4O_4S_2$: C, 70.42; H, 5.07; N, 4.27.

2.3 Crystallographic section. The structure presented herein was solved from a dark blue single crystal suitable for X-ray diffraction and obtained by slow diffusion of ethanol into a saturated dichloromethane solution of compound 1, at room temperature. Diffraction data were collected using a Rigaku MM007 HF copper rotating-anode generator with Osmic confocal optics and a rapid II Curved Image Plate at low temperature, 193 K. A total of 173 images with 5° rotation per image and two minute exposure per degree of oscillation were measured according to an ω-scan profile data strategy derived by the CrystalClear software package.[28] Intensities were integrated using FS_Process as implemented in the CrystalClear suite, then corrected for Lorentz-polarization effects, and scaled using symmetry-equivalent reflections using FS_Abscor. The structure was solved by direct methods (SHELXS-97)[29] and refined on F2 by means of full-matrix least-squares methods (SHELXL-97).[24] All non-hydrogen atoms were allowed anisotropic thermal motion. Aliphatic and aromatic C – H hydrogen atoms were included at calculated positions, with C – H = 0.98 Å, and 0.95 Å respectively and were refined with a riding model and with Uiso set to 1.5 (resp. 1.2) times that of the attached C atom. The structure showed the presence of three disordered dichloromethane solvent molecules with refined occupancy factors less than one but the overall modelling was not satisfactory, requiring resort to the SQUEEZE procedure of Spek and van der Sluis.[30] An extra 229 e/cell were indicated, corresponding to 2.7 molecules of CH_2Cl_2. Their contribution to the diffraction pattern was removed and modified Fo2 written to a new HKL file. The number of electrons thus located was included in the formula, formula weight, calculated density, µ and F(000). ORTEP drawings were made using ORTEP-III[31] as implemented within PLATON[29] and packing studies were carried out using MERCURY.[32]

The crystallographic data† are summarized as follows: dark blue prism of dimensions 0.44 x 0.18 x 0.12 mm, $C_{65}H_{48}BF_2N_4S_2$, 2.7 (CH_2Cl_2), M = 1354.20, triclinic, space group P -1, a = 12.6116 (5), b = 13.0839 (6), c = 20.2570 (14) Å, α = 80.833(6) °, β = 77.449(6) °, γ = 80.043(6)°, V = 3187.7(3) Å^3, Z = 2, Dcalcd =1.411 g/cm^3, F(000) = 1375, µ = 7.039 mm-1, 14957 collected reflections ($2.25° \le \theta \le 45°$), $-10 \le h \le 11$, $-12 \le k \le 12$, $-18 \le l \le 18$), 22781 independent reflections (Rint = 0.0481), goodness-of-fit on F^2: S = 1.188, R1 = 0.089 and wR2 = 0.209 for all 5140 reflections, R1 = 0.059 and wR2 = 0.168 for 5141 observed reflections [$I > 2\sigma(I)$], refining 676 parameters and 41 rigid-bond restraints (DELU with default esd), semi-empirical absorption correction from multi w-scans (Tmin = 0.20, Tmax = 0.46), final electron density between -0.386 and 0.418 eÅ^{-3}.

New Journal of Chemistry Accepted Manuscript

2.4 Device preparation. The OPV devices were fabricated on indium tin oxide (ITO) coated glass substrates (sheet resistance ~ 10 Ω/sq). The substrates were cleaned in an ultrasonic bath with de-ionized water, acetone, and methanol for 15 min, respectively. The 1-nm Ca layers were deposited onto ITO glass substrates in high vacuum chamber with base pressure of ~8×10-7 Torr, and the deposition were performed at a rate of 1~2 Å/s with the substrates held at room temperature. A blend solution of solar active Bodipy donors and $PC_{71}BM$ (purchased from Nano-C) were prepared using chloroform as solvent with different ratios and a total concentration of 15 mg/mL. The active layers were spin-coated on the substrates in a glove box under an anhydrous nitrogen atmosphere. The samples were then transferred to vacuum chamber for top electrode deposition. Devices were encapsulated using a UV-cured sealant (Everwide Chemical Co., Epowide EX) and a cover glass under the anhydrous nitrogen atmosphere after fabrication and were measured in air. The active area of the cells had an average size of 5 mm^2 (intersect area between Ag cathode and ITO anode) and were carefully measured device-by-device using calibrated optical microscope.

2.5 Characteristics measurement. Current density-voltage characteristics were measured with a SourceMeter Keithley 2400 under AM 1.5G simulated solar illumination from a xenon lamp solar simulator (Abet Technologies). The incident light intensity was calibrated as 100 mW/cm^2 using a NREL-traceable KG5 filtered Si reference cell. The external quantum efficiency (EQE) spectra were taken by illuminating chopped monochromatic light with a continuous-wave bias white light (from halogen lamp, intensity ~100 mW/cm^2) on the solar cells. The photocurrent signals were extracted with lock-in technique using a current preamplifier (Stanford Research System) followed by a lock-in amplifier (AMETEK). The EQE measurement is fully computer controlled and the intensity of monochromatic light is carefully calibrated with NIST-traceable optical power meter (Ophir Optronics). Thicknesses and extinction coefficients (k) of the thin films were determined using spectroscopic ellipsometry (J. A. Woollam Inc. V-VASE). Atomic force microscopy (AFM) images were taken with Veeco Nanoscope 3100 atomic force microscope. The electron and hole mobilities for the BODIPY:PC71BM blended films were carried out by using SCLC method. The hole only device was configured as follows: ITO/MoO_3 (1 nm)/Bodipy:$PC_{71}BM$ (80 nm)/MoO_3 (10 nm)/Al (80 nm), while the electron only device was configured as follows: ITO/Mg (5 nm)/Bodipy:$PC_{71}BM$ (80 nm)/Ca (5 nm)/Al (80 nm). Current density-voltage characteristics of SCLC devices were also measured with a SourceMeter Keithley 2400. The annealing process was performed by placing the encapsulated devices on a temperature controlled hot plate.

3 Results and discussion

3.1 Synthesis and characterization

The synthetic protocol used to prepare the novel dyes is sketched in Scheme 1. The first step produced compound **A** by cross-coupling of 4-(bromophenyl)diphenylamine and 2-trimethyltinthiophene. Formylation of **A** under Vilsmeier-Haack conditions provided regio-selectively the aldehyde **B** in excellent yield under mild conditions. Next, a Knoevenagel reaction using forcing conditions provided the deep-green divinyl derivative **1** in an average yield of 86%. The use of the Grignard reagent of 3-(2-methoxyethoxy)prop-1-yne provided dye **2** in about 75%. All compounds were purified by column chromatography. The molecular structures were assigned by NMR spectroscopy, elemental analysis and mass spectroscopy and these data unambiguously confirm those assigned. Proton NMR spectra were diagnostic for the state of boron substitution. It has been clearly established that by boron substitution with an ethynyl residue the vinyl protons ***a*** (2H) at 8.02 ppm (J_{H-H} = 16 Hz) are deshielded in **2** by 0.54 ppm, compared to the same protons at 7.48 ppm in the BF_2 compound **1**. In contrast, the doublet at 7.86 ppm (2H, J_{H-H} = 8 Hz) assigned to the AB quartet of the phenyl proton ***b*** in the pseudo meso position remained unchanged in both compounds (Figure 1). Furthermore, the high coupling constants (J_{H-H} = 16 Hz) for the vinylic protons are in keeping with a *trans* conformation of the double bonds. Finally, the β-pyrrolic protons ***c*** remains unchanged at 6.6 ppm.

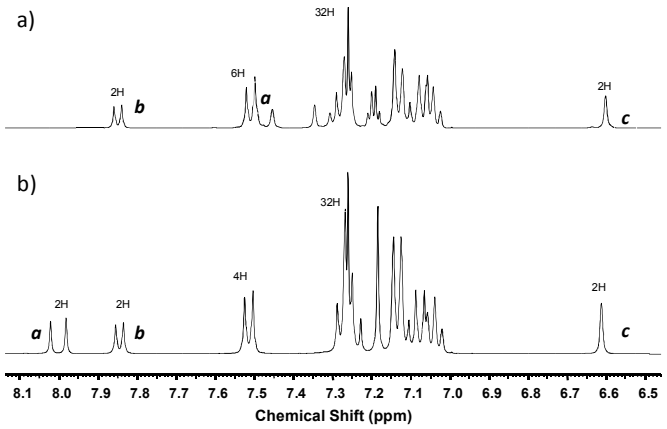

Figure 1. Partial ^1H NMR spectra of dye **1** a) and dye **2** b) in $CDCl_3$ at rt.

3.2 X-ray characterization

X-ray diffraction on a blue single crystal confirms that the structure of compound **1** shown in Figure 2 incorporates a nearly flat 3,5-vinylbisthienyl-Bodipy framework as recently described elsewhere[19] in a related compound (see Figure 3): it features an even more nearly-planar Bodipy platform (maximum deviation from the mean least-squares plane is 0.107 (8) Å for the carbon atom C5) and a near-orthogonally-attached (89.0°) iodobenzene group with ∠ C9 B1 I1 of 4.2 °.

New Journal of Chemistry Accepted Manuscript

This journal is © The Royal Society of Chemistry 2012

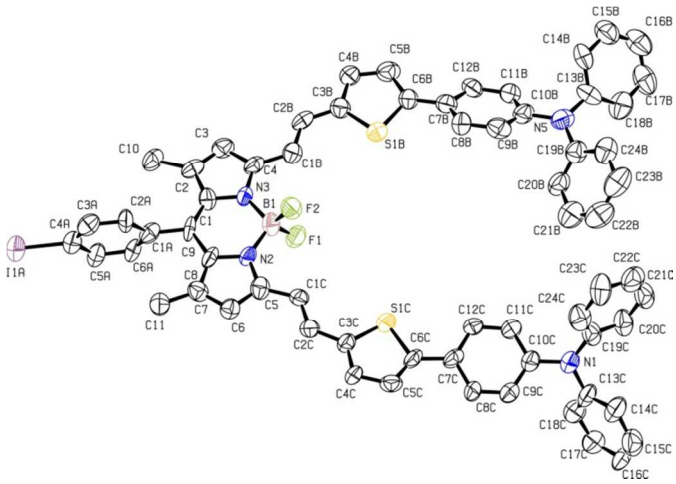

Figure 2. ORTEP view of compound **1**. Thermal ellipsoids are plotted at the 30% level. B1–N3, B1–N2, B1–F1, B1–F2, N3–C1, N2–C8, N3–C4 and N2–C5 bond lengths are 1.525(14), 1.516(14), 1.376(14), 1.389(13), 1.370(10), 1.370(10), 1.349(11) and 1.368(11) Å, respectively and the FB–F, N–B–F, and N–B–N angles are 107.2(10), 111.0(11) /110.9(11) /110.6(10)/109.2(10) and 107.9(10)°.

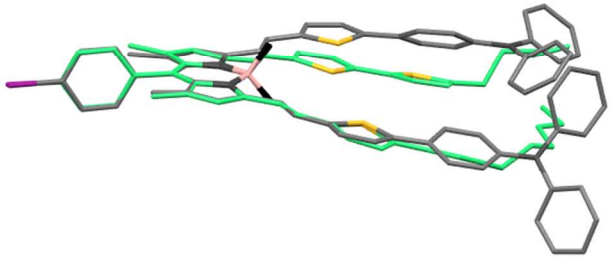

Figure 3. A superposition of the compound **1** and compound 3,5-vinylbisthienyl-Bodipy[18] (in green) generated by least-squares fitting of their iodophenyl-Bodipy groups.

Similarity extends to the sulphur atoms from the first thiophene groups of both arms, which face one another. In the crystal, the flat molecules assemble in a layered structure, parallel to the plane (3 3 -4) with an interplanar separation of 3.50 ± 0.06 Å (Figure 4). Within a layer, the V-shaped molecules are aligned along the [1 0 -1] direction with the iodophenyl group pointing here towards a phenyl from the triphenylamine unit of one of the two arms, unlike the former complex crystal structure in which iodobenzene group was inserted between the arms of a neighbor, interacting with the BF_2 group. As a direct consequence, this interaction maintains the thiophene and the phenyl ring bonded to it coplanar with Bodipy platform whereas the other arm is tilted from the mean plane by an angle of circa 9.5°. The triphenylamine unit in interaction with the iodo atom adopts a close to staggered conformation with respect to the mean plane, with the outer phenyl groups interposed between molecular layers. This contrasts with the other triphenylamine unit, where with the phenyl groups are oriented in an eclipsed way. Relative to the mean plane defined by the N atom and its three bound C atoms, the torsion angles of each of the aromatic rings range from 28 .6 to 43.3° for the latter group and from 38.6 to 45.0° for the former one, but are similar to the values observed for the diphenylaminophenyl units, 37.0 (7) ≤ ≤ 50.5 (7)°.[33] Between adjacent layers, inversion related molecules at general position and at 2-x,1-y,1-z lie pairwise head-to-tail, the Bodipy platform lying over the inside phenyl of the 'flat', eclipsed triphenylamine unit, with the arms overlapped and an S···S distance of 4.03 Å. As well, π – π stacking interactions occur where the molecules at 1-x, 1-y, 1-z and 2-x, -y, 1-z in one layer extend one arm towards their equivalent molecule in next layer, resulting in thiophene groups overlapping the outer five-membered ring of the Bodipy with a centroid-centroid distance of 3.69 ± 0.03 Å (Figure 5).

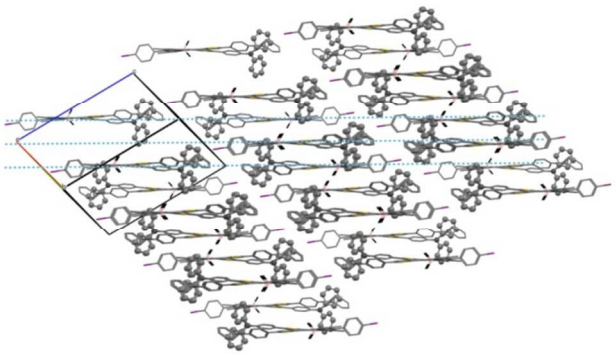

Figure 4. Lattice view highlighting the layered structure parallel to the (3 3 -4) plane (cyan dotted lines). Phenyl units from the triphenylamine substituents interspersed between the layers are shown as balls.

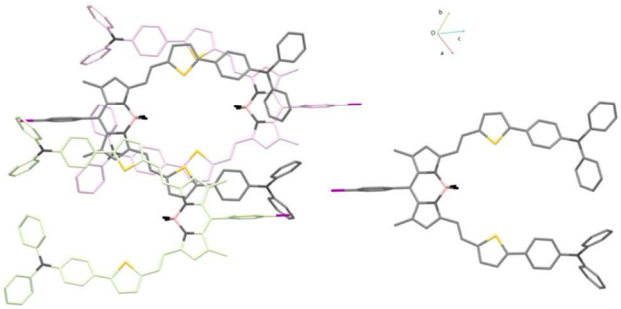

Figure 5. Part of the crystal structure viewed down the molecular stacking direction. Molecules from n-1, n and n+1 layers are in pink, grey and light green respectively.

3.3 Spectroscopic characterization.

Dyes **1** and **2** display similar spectroscopic features (Figure 6) in THF, with three intense absorption peaks in the 350-550 nm and 600-750 nm range and extinction coefficients of about 70,000 $M^{-1}cm^{-1}$ for the former peaks and 90,000 $M^{-1}cm^{-1}$ for the latter. The higher energy transition at 391 nm is due to the styryl fragments,[34] while that at 719 nm is the $S_0 \rightarrow S_1$ transition of the Bodipy core with a clear vibronic sequence ($\Delta\nu$ = 1100 cm^{-1}) characteristic of the dipyrromethene framework. The unusual transition observed at 462 nm is not present in most of the styryl derivatives,[33] but present when dimethylamino residues are used for the construction of the dye, and has been assigned to a charge transfer transition.[35] Weak fluorescence at 767 nm for **1** and 758 nm for **2** was detected with an estimated

New Journal of Chemistry Accepted Manuscript

quantum yield of around 3 to 4%. This fluorescence is independent from the excitation wavelength and in both cases the excitation spectra perfectly match the absorption spectra, excluding the presence of aggregates (Figure 6). The thin-film (thickness of about 50 nm) absorption spectra of **1** and **2** exhibit red-shifts, with λ_{max} = 766 nm and 760 nm, respectively (Figure 7). The red-shift and broadened absorption is possibly due to the π-π interaction in the solid state as seen in the crystal packing. The broad thin-film absorption of **1** and **2** which covers the photo-harvesting range from UV to near-IR is promising for application in photovoltaic devices. Optical constants for **1** and **2** thin films are shown in Figure 8. The extinction coefficients, *k*, are consistent with the absorption spectra with high values from 300 nm to 800 nm.

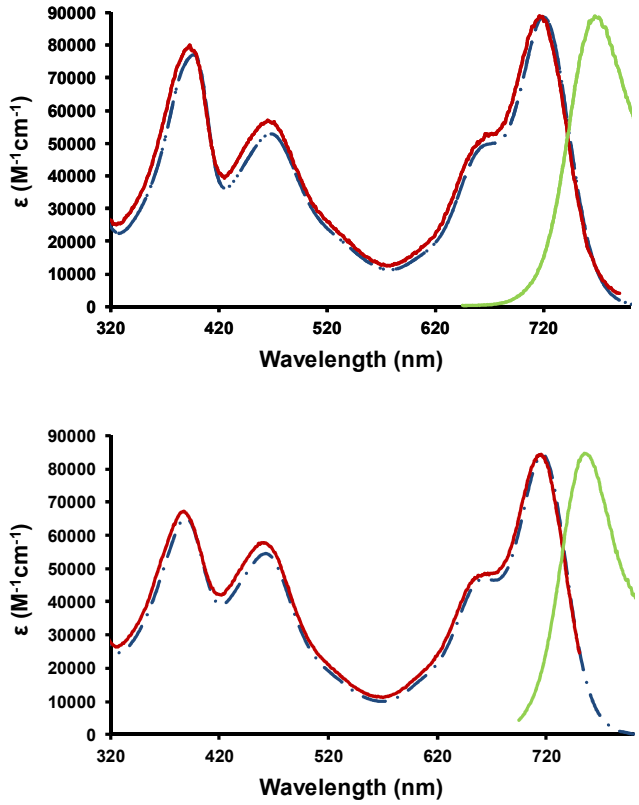

Figure 6. Absorption (blue trace), emission (green trace) and excitation spectra (red traces) of dye **1** at λ_{exc} @ 640 nm and λ_{em} @ 800 nm (a) and dye **2** (b) at λ_{exc} @ 650 nm and λ_{em} @ 780 nm in THF, at rt.

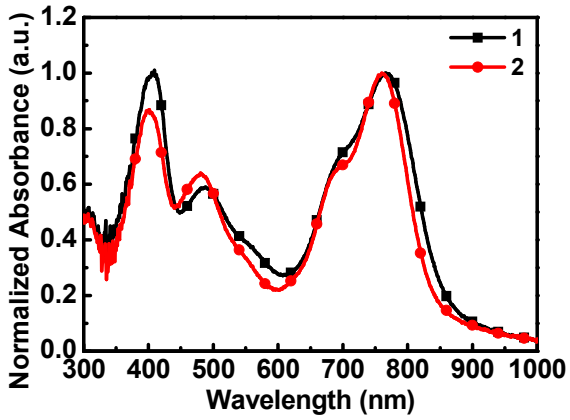

Figure 7. Thin-film absorption spectra of **1** and **2**.

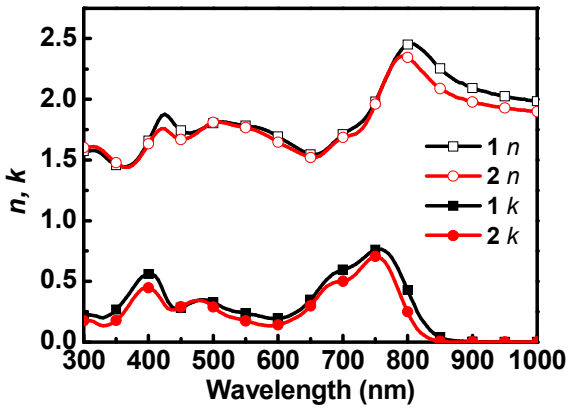

Figure 8. Optical constants (refractive index, *n*, and extinction coefficient, *k*) of **1** and **2** thin films.

3.4 Redox properties.

Cyclic voltammetry was used to determine the HOMO/LUMO levels of the dyes in solution, with $PC_{61}BM$ and ferrocene used as calibrants. Ferrocene is used because its Fermi level in the vacuum is well-known and $PC_{61}BM$ because this acceptor is used in the real solar cell device. Owing to the low solubility of $PC_{71}BM$ in dichloromethane, $PC_{61}BM$ was preferred for the calibration. Under similar conditions but at low concentration (about 10^{-4} M) and at 40°C, $PC_{71}BM$ is easier to reduce than $PC_{61}BM$ by 120 mV. Both dyes display a rich electrochemistry induced by the presence of various electroactive modules (Table 1, Figure 9). For both dyes, two reversible oxidation waves at about +0.60 V and +1.00 V were observed. The first of these waves is dielectronic whereas the second process is monoelectronic. No splitting of the waves was observed for dye **1** whereas for the more bulky dye **2** the first oxidation wave was clearly split into two waves at +0.54 and +0.62 V (Figure 9a). In light of previous electrochemical studies achieved with similar thienyl-derivatives (**D** and **E** in Chart I) engineered

New Journal of Chemistry Accepted Manuscript

This journal is © The Royal Society of Chemistry 2012

from styryl-derivatives, it clearly appeared that the first oxidative redox potential is assigned to one pyrrole-vinyl-thiophene arm while the second potential (usual similar or very close to the first potential) is assigned to the second pyrrole-vinyl-thiophene arm. In case of dissymmetric side-arms (eg **F** in Chart I), two distinguish potentials are clearly observed.[19,36] We have previously observed that the shifts of these redox potential reflects the differing degrees to which the principal donor couples to the extended Bodipy unit.[37] DFT calculations indicate that both HOMO and HOMO(-1) are spread over much of the molecule and include contributions from the Bodipy and donor residues. As such, it is inaccurate to ascribe the first oxidation step as being localized on either the TPA or the Bodipy unit.

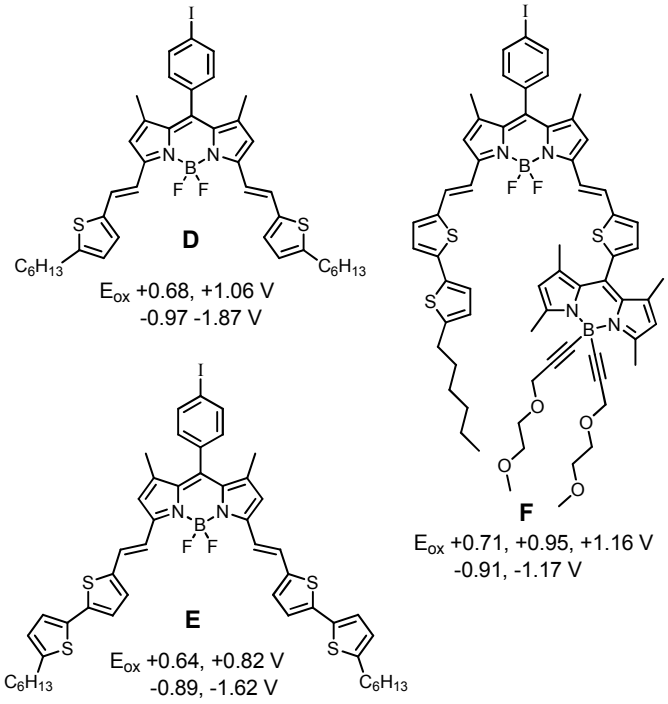

Chart I. Various thienyl-Bodipy derivatives extracted from references 18 (for D and E) and 35 (for F).

In both cases, two reduction waves were observed around -1.00 V typical of radical anion formation on the Bodipy core and a second irreversible wave observed around -1.70 V was assigned to the Bodipy dianion.[38] Interestingly, when compared with related dyes e.g. 3,5-vinylbisthienyl-Bodipy **B**[19] and as would be expected by the fact that TPA fragment imports additional electronic density, the first oxidation potential in the novel dyes were cathodically shifted (easier oxidation) by 50 and 100 mV respectively for **1** and **2**. Whereas, the reduction potentials were anodically shifted (more difficult reduction) by 70 mV and 180 mV respectively for **1** and **2**. Notice that there is a significant driving force (about 0.25 eV) for photoinduced electron transfer from the photoexcited dyes toward $PC_{61}BM$ (Figure 9b). With the exception of the last reduction potential, all redox processes were highly reversible ($i_{pa}/i_{pc} \approx 1$) and exhibited the characteristic shape (ΔE_p = 60-70 mV) of a Nernstian process.

Table 1. Electrochemical data for relevant compounds.[a)]

Dyes	$E^{0'}$(ox, soln) (V), ΔE (mV)	$E^{0'}$(red, soln) (V), ΔE (mV)	Electro-gap (eV)	Optical-gap (eV)[b)]
1	+0.59 (70), +1.03 (70)	-0.96 (70), -1.73 (irr.)	1.55	1.58
1 + PCBM*	+0.59 (70), +1.03 (70)	-0.70 (60)*, -0.96 (70)*, -1.08 (70), -1.59 (70)*, -1.80 (irr.)	-	-
2	+0.54 (60) , +0.62 (70), +0.99 (60),	-1.07 (60), -1.80 (irr.)	1.61	1.62
2+PCBM*	+0.54 (60) , +0.62 (70), +0.99 (60),	-0.70 (60)*, -0.95 (70)*, -1.07 (60), -1.58 (70)*, -1.78 (irr.)	-	-

a) Potentials determined by cyclic voltammetry in deoxygenated dichloromethane solution, containing 0.1 M $TBAPF_6$, [electrochemical window from +1.7 to -2.2 V], at a solute concentration of ca. 1.5 mM and at rt. Potentials were standardized versus ferrocene (Fc) as internal reference and converted to the SCE scale assuming that $E_{1/2}$ (Fc/Fc^+) = +0.38 V (ΔEp = 60 mV) *vs* SCE. Error in half-wave potentials is ±10 mV. For irreversible processes the peak potentials (E_{ap}) are quoted.
b) Determined from the absorption spectra from the onset with the tangent at the low energy side.

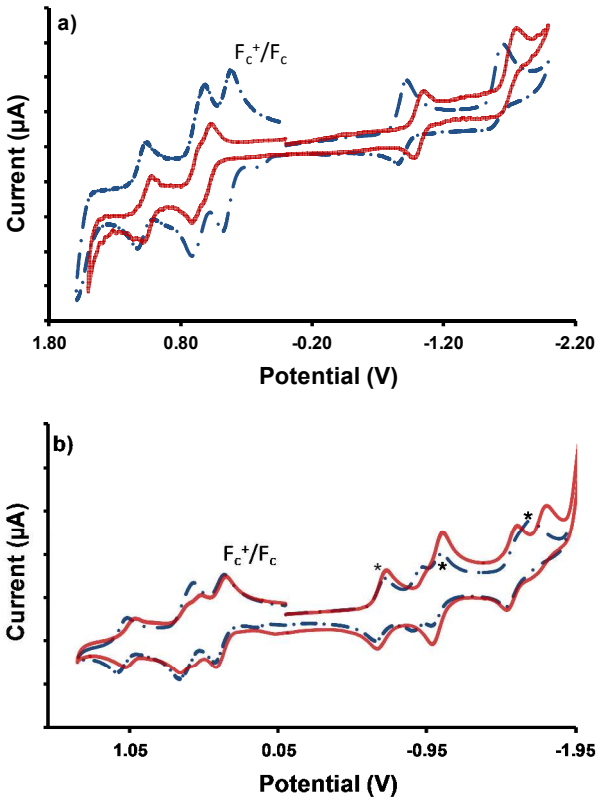

Figure 9. Cyclic voltammetry of : a) Dye **1** with ferrocene at 0.38 V (blue dashed line) and **2** (red continous line); b) Dye **1** calibrated with ferrocene and $PC_{61}BM$ (blue dashed line) and **2** with ferrocene and $PC_{61}BM$ (red continous line). Fc accounts for ferrocen and * for $PC_{61}BM$.

3.5 Solar cells and characterization

Ultraviolet photoelectron spectroscopy in air was utilized to measure the energy levels of **1** and **2** in the thin-film state (Figure S1). The HOMO levels of **1** and **2** were found to be -5.14 eV and -5.02 eV, respectively. These values together with the HOMO/LUMO gap estimated from the absorption spectra were used to acquire the LUMO levels of the compounds (-3.50 eV for **1** and -3.37 eV for **2**). The LUMO levels of these

New Journal of Chemistry Accepted Manuscript

compounds are at least 0.2 eV higher than those of fullerenes (-3.7 to -4.3 eV), ensuring efficient charge transfer between **1** and **2** with fullerenes under irradiation.

For photovoltaic characterization, we adopted the inverted structure utilizing ultra-thin 1 nm Ca as a cathode and MoO_3 as a hole extraction layer. The structure has been used in our previous Bodipy cells and showed promising performance.[19c] The optimized device structure was configured as follows: ITO/Ca (1 nm)/**1** or **2**:$PC_{71}BM$ (~80 nm)/MoO_3 (7 nm)/Ag (150 nm). The details of optimization are provided in the experimental part. The active layers of the devices were spin-cast from a chloroform solution of the mixture of Bodipy dyes and $PC_{71}BM$. Figure 10 shows the current density to voltage (J-V) characteristics and the corresponding external quantum efficiencies (EQEs) of the **1**:$PC_{71}BM$ cells. There is negligible difference in the V_{oc} value in the cells with various donor to acceptor ratios (Table 2). However, the J_{sc} and EQE values increased significantly with the increase of $PC_{71}BM$ ratio. The best cell with **1**:$PC_{71}BM$ = 1:1.5 showed V_{oc} of 0.71 V, J_{sc} of 5.5 mA/cm^2, fill factor (FF) of 0.31 and overall PCE of 1.2%. Figure 11 shows the J-V and EQE characteristics of the **2**:$PC_{71}BM$ cells. The V_{oc}, FF and PCE are lower than that of **1**:$PC_{71}BM$ devices. However, as shown in Figure 12, interestingly, upon annealing the devices at 150 °C for 10 min, the **1**:$PC_{71}BM$ cell showed no difference from the device without annealing, but J_{sc} and PCE were considerably increased in the **2**:$PC_{71}BM$ devices. This can be rationalized by the carrier mobility in the active layers. The carrier transportation properties were investigated using space-charge-limited-current (SCLC) method. As shown in Figure 13, the hole mobilities in the BHJ were all increased after annealing. In the **2**:$PC_{71}BM$ thin film, the electron and hole mobilities were initially very unbalanced. Nevertheless, after thermal annealing, the hole mobility was enhanced by 2 orders of magnitude and matched the mobility of electrons. On the other hand, the **1**:$PC_{71}BM$ thin film exhibited balanced mobilities without thermal annealing. This may explain why the performance of the **2**:$PC_{71}BM$ devices increased upon annealing while that of the **1**:$PC_{71}BM$ cell remained constant.

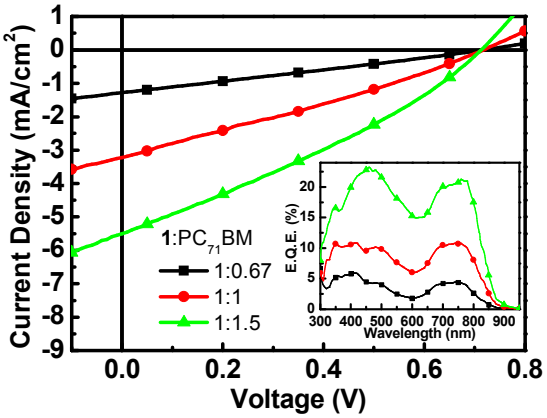

Figure 10. Current density-voltage characteristics (under AM 1.5G, 100mW/cm^2 illumination) and EQE spectra (inset) of the **1**:$PC_{71}BM$ devices.

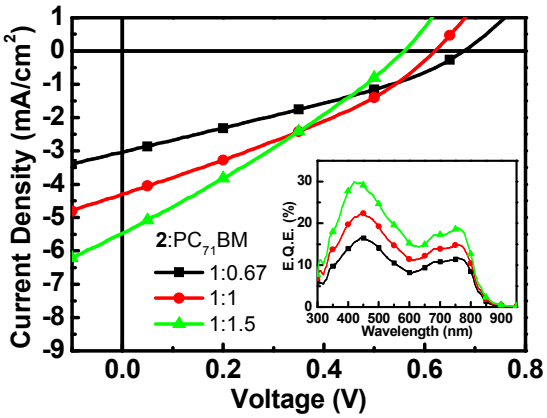

Figure 11. Current density-voltage characteristics (under AM 1.5G, 100mW/cm^2 illumination) and EQE spectra (inset) of the **2**:$PC_{71}BM$ devices.

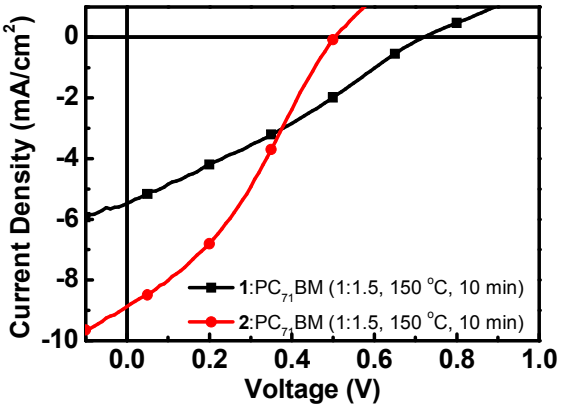

Figure 12. Current density-voltage characteristics of the **1**:$PC_{71}BM$ and **2**:$PC_{71}BM$ devices after annealing for 10 min at 150 °C.

Table 2. Performance parameters of devices.

Device	V_{OC} (V)	J_{SC} (mA/cm^2)	FF	PCE (%)
1: $PC_{71}BM$ (1:0.67)	0.72	1.3	0.26	0.24
1: $PC_{71}BM$ (1:1)	0.72	3.2	0.28	0.65
1: $PC_{71}BM$ (1:1.5)	0.71	5.5	0.31	1.2
2: $PC_{71}BM$ (1:0.67)	0.68	3.0	0.30	0.61
2: $PC_{71}BM$ (1:1)	0.62	4.3	0.32	0.85
2: $PC_{71}BM$ (1:1.5)	0.56	5.5	0.29	0.89
1: $PC_{71}BM$ (1:1.5)[a]	0.72	5.5	0.29	1.1
2: $PC_{71}BM$ (1:1.5)[a]	0.51	8.9	0.34	1.5

[a] 150 °C annealing for 10 mins.

New Journal of Chemistry Accepted Manuscript

This journal is © The Royal Society of Chemistry 2012

4 Conclusions

In short, we have synthesized new green Bodipy dyes incorporating two thienyl-vinyl units bridging a Bodipy core with two 4-diphenylamino-phenyl fragments at the wings. This is an original strategy which does not required post-functionalization of the dyes. The X-ray structure of one of these dyes shows that the main part of the molecule is flat but that its iodophenyl substituent ring is quasi orthogonal (89°) with the main core and that the molecules pack into layers 3.5 Å apart involving π-π and S···S interactions. In the electronic absorption spectra, a new charge transfer band appears around 460 nm due to interaction between the strong "push" units at the periphery and the central Bodipy "pull" unit. This is an interesting approach which also contributes to the increase of photon absorption either in solution or in the thin film. This strong absorption and redox activity of these dyes enable the preparation of bulk heterojunction with thin films blended with $PC_{71}BM$ which produce a photocurrent reflecting the absorption of the dye in the films. Promising efficiencies around 1.5% were obtained. We note that the synthetic routes outlined here provide the scope to further tune the performance of the solar cells by postfunctionalization of the phenyl-iodo moiety with electron attractor modules or substituents suitable to promote supramolecular interactions with the electron acceptor.

Acknowledgements

We thank the Centre National de la Recherche Scientifique (CNRS) for financial support of this work. Professor Jack Harrowfield (ISIS in Strasbourg) is warmly acknowledged for a critical reading of this manuscript prior to publication.

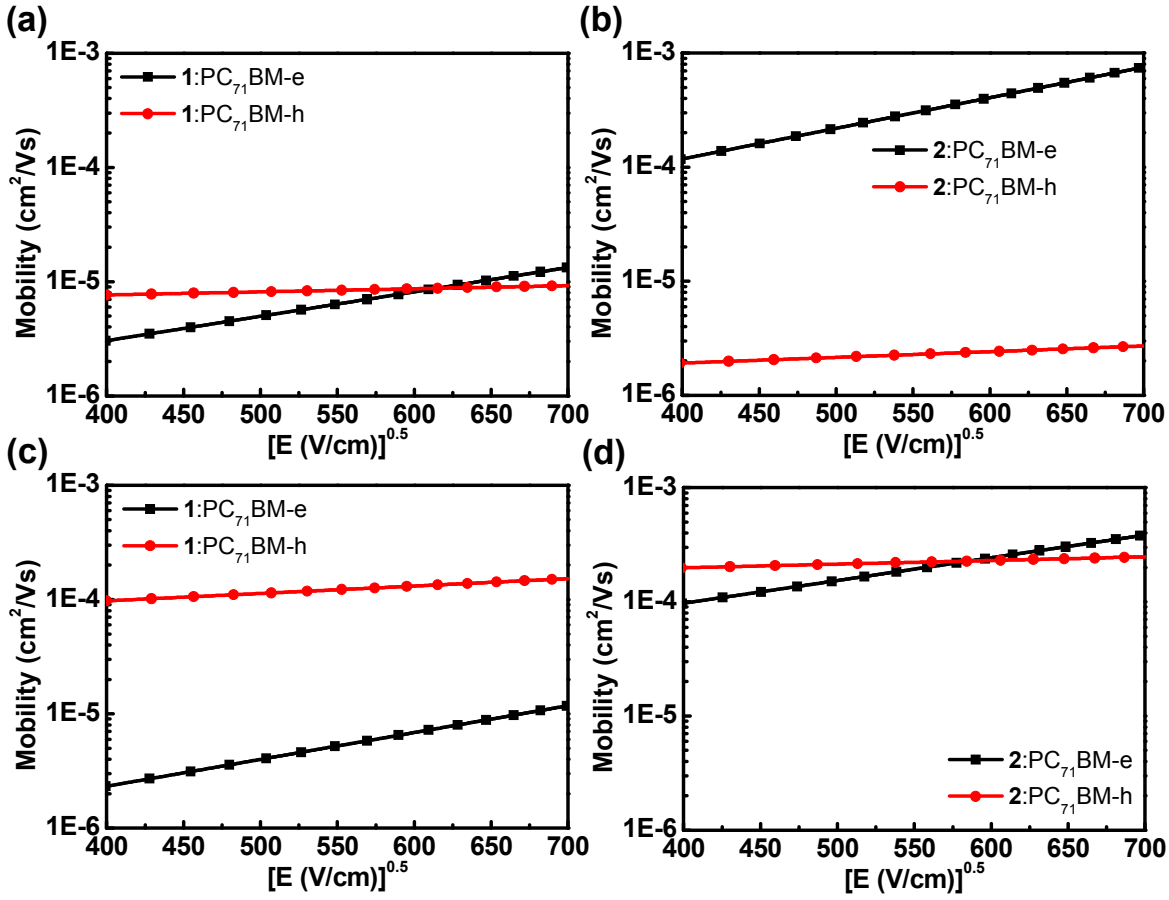

Figure 13. Carrier mobility of (a) **1**:$PC_{71}BM$, (b) **2**:$PC_{71}BM$ BHJ without annealing and (c) **1**:$PC_{71}BM$, (d) **2**:$PC_{71}BM$ BHJ after annealing for 10 min at 150 °C.

New Journal of Chemistry Accepted Manuscript

Graphical Abstract

Original Flat Push-Pull-Push Dyes have been engineered from thienyl-Bodipy-triphenylamine frameworks for solar cells application.

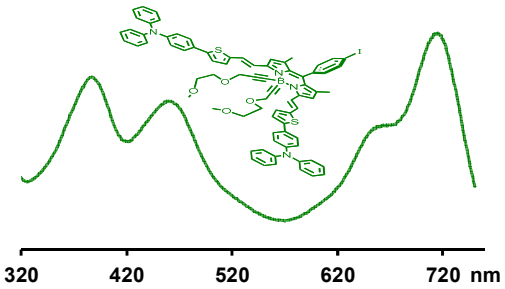

Notes and references

[a] Laboratoire de Chimie Organique et Spectroscopies Avancées (ICPEES-LCOSA), UMR 7515 au CNRS, Ecole Européenne de Chimie, Polymères et Matériaux, Université de Strasbourg, 25 rue Becquerel, 67087 Strasbourg Cedex 02, France
[b] Centre de Recherche de Gif, Institut de Chimie des Substances Naturelles, UPR2301-CNRS, Bâtiment 27, 1 avenue de la Terrasse, 91198 Gif sur Yvette Cedex, France
[c] Department of Materials Science and Engineering, National Tsing Hua University, Hsinchu, Taiwan

† CCDC 939187 (compound **1**) contains the supplementary crystallographic data. These data can be obtained free of charge via www.ccdc.cam.ac.uk/conts/retrieving.html (or from the Cambridge Crystallographic Data Centre, 12 Union Road, Cambridge CB2 1EZ, UK; fax: (+44) 1223-336033; or deposit@ccdc.cam.uk). Electronic Supplementary Information (ESI) available: [details of any supplementary information available should be included here]. See DOI: 10.1039/b000000x/

[1] a) N. S. Lewis and D. G. Nocera, *Proc. Natl. Acad. Sci. USA* 2006, **103**, 15729-15735. b) N. Armaroli and V. Balzani, *Angew. Chem. Int. Ed*. 2007, **46**, 52-66. c) J. Liu, G. Cao, Z. Yang, D. Wang, D. Dubois, X. Zhou, G. L. Graff, L. R. Pederson and J.-G. Zhang, *ChemSusChem*. 2008, **1**, 676-697.

[2] In *Organic Photovoltaïcs : Materials, Device Physics, and Manufacturing Technologies* ; C. Brabec, V. Dyakonov and U. Scherf Eds.; Wiley-VCH: Weinheim, Germany, 2008.

[3] L Dou, J. You, J. Yang, C.-C. Chen, Y. He, S. Murase, T. Moriarty, K. Emery, G. Li and Y. Yang, *Nat. Photonics* 2012, **6**, 180-185.

[4] a) S. Berson, R. D. Bettignies, S. Bailly and S. Guillerez, *Adv. Funct. Mater*. 2007, **17**, 1377-1384. b) C. W. Chu, H. Yang, W. J. Hou, J. Huang, G. Li and Y. Yang, *Appl. Phys. Lett*. 2008, **92**, 103306-1-10330-3.

[5] a) J. Zhou, X. Wan, Y. Liu, Y. Zuo, Z. Li, G. He, G. Long, W. Ni, C Li, X. Su and Y. Chen, *J. Am. Chem. Soc*. 2012, **134**, 16345-16351. b) T. S. van der Poll, J. A. Love, T.-Q. Nguyen and G. C. Bazan, *Adv. Mater*. 2012, **24**, 3646-3649. c) A. K. K. Kyaw, D. H. Wang,D. Wynands, J. Zhang, T.-Q. Nguyen, G. C. Bazan and A. J. Heeger, *Nano Lett*. 2013, **13**, 3796-3801.

[6] Heliatek GmbH ; press release on http://www.heliatek.com.

[7] G. Yu, J. Gao, J. C. Hummelen, F. Wudl and A. J. Heeger, *Science*, 1995, **270**, 1789-1791.

[8] (a) R. Fitzner, E. Reinold, A. Mishra, E. Mena-Osteritz, H. Ziehlke, C. Körner, K. Leo, K.; M. Riede, M. Weil, O. Tsaryova, A. Weiss, C. Uhrich, M. Pfeiffer and P. Bäuerle, *Adv. Funct. Mater*. 2011, **21**, 897-910. (b) R. Fitzner, E. Mena-Osteritz, A. Mishra, G. Schulz, E. Reinold, M. Weil, C. Körner, H. Ziehlke, C. Elschner, K. Leo, M. Riede, M. Pfeiffer, C. Uhrich, and P. Bäuerle, *J. Am. Chem. Soc*. 2012, **134**, 11064-11067.

[9] B. Walker, A. B. Tamayo, X.-D. Dang, P. Zalar, J. H. Seo, A. Garcia, M. Tantiwiwat and T.-Q. Nguyen, *Adv. Funct. Mater.* 2009, **19**, 3063-3069.

[10] T. Bura, N. Leclerc, R. Bechara, P/ Lévêque, T. Heiser and R. Ziessel, *Adv. Energy Mater*. 2013, **3**, 1118-1124.

[11] a) G. Wei, S. Wang, K. Sun, M. E. Thompson and S. R. Forrest, *Adv. Eng. Mater*. 2011, **2**, 184-187. b) A. Ajayaghosh, *Acc. Chem. Res*. 2005, **38**, 449-459.

[12] W. W. H. Wong, T. B. Singh, D. Vak, W. Pisula, C. Yan, X. Feng, E. L. Williams, K. L. Chan, Q. Mao, D. J. Jones, C.-Q. Ma, K. Müllen, P. Baüerle and A. B. Holmes, *Adv. Funct. Mater*. 2010, **20**, 927-938.

New Journal of Chemistry Accepted Manuscript

 This journal is © The Royal Society of Chemistry 2012

[13] N. M. Kronenberg, M. Deppisch, F. Würthner, H. W. A. Ladermann, K. Deing and K. Meerholz, *Chem. Commun*. 2008, 6489-6491.
[14] H. Bürckstümmer, E. V. Tulyakova, M. Deppisch, M. R. Lenze, N. M. Kronenberg, M. Gsänger, M. Stolte, K. Meerholz and F. Würthner, *Angew. Chem. Int. Ed*. 2011, **45**, 11628-11632.
[15] Y. Sun, G. C. Welch, W. L. Leong, C. J. Takacs, G. C. Bazan and A. J. Heeger, *Nature Mater*. 2011, **11**, 44-48.
[16] J. Zhou, X. Wan, Y. Liu, Y. Zuo, Z. Li, G. He, G. Long, W. Ni, C Li, X. Su and Y. Chen, *J. Am. Chem. Soc*. 2012, **134**, 16345-16351.
[17] Y.-H. Chen, L.-Y. Lin, C.-T. Lun F. Lin, Z.-Y. Huang, H.-W. Lin, P.-H. Wang, Y.-H. Liu, K.-T. Wong, J. Wen, D. J. Miller and S. B. Darling, *J. Am. Chem. Soc*. 2012, **134**, 13616−13623.
[18] a) T. Rousseau, A. Cravino, T. Bura, G. Ulrich, R. Ziessel and J. Roncali, *Chem. Commun*. 2009, 1673-1675. b) T. Rousseau,. A. Cravino, T. Bura, G. Ulrich, R. Ziessel and J. Roncali*, J. Mater. Chem*., 2009, **19**, 2298–2300. c) T. Rousseau, A. Cravino, E. Ripaud, P. Leriche, S. Rihn, A. De Nicola, R. Ziessel and J. Roncali, *Chem. Commun*. 2010, **46**, 5082-5084.
[19] T. Bura, N. Leclerc, S. Fall, P. Lévêque, T. Heiser, P. Retailleau, S. Rihn, A. Mirloup and R. Ziessel, *J. Am. Chem. Soc*. 2012, **134**, 17404−17407.
[20] a) B. S. Kim, B. Ma, V. R. Donuru, H. Liu and J. M. J. Fréchet *Chem. Commun*. 2010, **46**, 4148. b) T. Bura, N. Leclerc, S. Fall, P. Lévêque, T. Heiser and R. Ziessel, *Org. Lett*. 2011, **13**, 6030-6033. c) H.-Y.Lin, W.-C. Huang, H.-H. Chou, C.-Y. Hsu, J. T. Lin and H.W. Lin, *Chem. Commun*. 2012, **48**, 8913-8915.
[21] (a) S. Hattori, K. Ohkubo, Y. Urano, H. Sunahara, T. Nagano, Y. Wada, N. V. Tkachenko, H. Lemmetyinen, and S. Fukuzumi, *J. Phys. Chem. B*, 2005, **109**, 15368-15375; (b) S. Erten-Ela, M. D. Yilmaz, B. Icli, Y. Dede, S. Icli and E. U. Akkaya *Org. Lett*., 2008, **10**, 3299-3302; (c) D. Kumaresan, R. P. Thummel, T. Bura, G. Ulrich, and R. Ziessel, *Chem.–Eur. J*., 2009, **15**, 6335-6339; (d) S. Kolemen, Y. Cakmak, S. Erten-Ela, Y. Altay, J. Brendel, M. Thelakkat and E. U. Akkaya, *Org. Lett*., 2010, **12**, 3812-3815.
[22] (a) R. Ziessel, G. Ulrich and A. Harriman, *New J. Chem*. 2007, **31**, 496-501. (b) G. Ulrich, R. Ziessel and A. Harriman, *Angew. Chem. Int. Ed*. 2008, **47**, 1184-1201.
[23] J. H. Olivier, J. Barbera, E. Bahaidarah. A. Harriman and R. Ziessel *J. Am. Chem. Soc*. 2012, **134**, 6100-6103.
[24] G. Ulrich, S. Goeb, A. De Nicola, P. Retailleau and R. Ziessel *Synlett*. 2007, 1517-1520.
[25] D. R. Coulson, L. C. Satek and S. O. Grim, *Inorg. Synth.*, 1972, **13**, 121-124.
[26] G. Qian, B. Dai, M. Luo, D. Yu, J. Zhan, Z. Zhang, D. Ma and Z. Y. Wang, *Chem. Mater*, 2008, **20**, 6208-6216.
[27] A. Leliège, C.-H. Le Régent, M. Allain, P. Blanchard and J. Roncali*, Chem. Commun*., 2012, **48**, 8907-8909.
[28] CrystalClear-SM Expert 2.0 r4 (Rigaku, 2009).
[29] G. M. Sheldrick, *Acta Cryst., Sect. A,* 2008, **64**, 112-122. R. Welter, *Acta Cryst.* 2006, **A62**, S252-S254.
[30] A. L. Spek, *J. Appl. Cryst.* 2003, **36**, 7-13.
[31] M. N. Burnett and K. J. Carroll, Oak Ridge National Laboratory Report ORNL-6895,1996.
[32] C. F. Macrae, P. R. Edgington, P. McCabe, E. Pidcock, G. P. Shields, R. Taylor, M. Towler and J. van de Streek, J., *J. Appl. Cryst.*, 2006, **39**, 453-457.
[33] A. N. Sobolev, V. K. Belsky, I. P. Romm, N. Yu. F. Chernikova and E. N. Guryanova, *Acta Cryst.* 1985, **C41**, 967-971.
[34] R. Ziessel, T. Bura and J.-H. Olivier, *Synlett,* 2010, 2304-2310.
[35] R. Ziessel, G. Ulrich, A. Harriman, M. A. H. Alamiry, B. Stewart and P. Retailleau, *Chem.–Eur. J*., 2009, **15**, 1359-1369.
[36] A. Mirloup and R. Ziessel, Tet. Letters 2013, 54, 4456-4462.
[37] A. Nano, R. Ziessel, P. Stachelek and A. Harriman, Chem. Eur. J. 2013, 19, 13528-13537.
[38] R. Ziessel, L. Bonardi, P. Retailleau and G. Ulrich, *J. Org. Chem*., 2006, **71**, 3093-3102.

New Journal of Chemistry Accepted Manuscript